Supplementary Information (SI) for Green Chemistry.

Supporting Information

Regulation of lithium ion transport dynamics via carbonized-polymer-dots modified substrate to achieve 2 mV ultralow voltage hysteresis

Jiayu Zhang[a 1], Yanfei Li[b 1], Yihan Song[a], Guoduo Yang[a], Zhuo Wang[a], Xinyao Huang[a], Haizhu Sun[a]*

[a]*College of Chemistry, National & Local United Engineering Laboratory for Power Batteries*

Northeast Normal University

No. 5268, Renmin Street, Changchun, 130024, P. R. China
E-mail: sunhz335@nenu.edu.cn

[b]*State Key Laboratory of Organic Electronics and Information Displays & Institute of Advanced Materials (IAM), School of Chemistry and Life Sciences*

Nanjing University of Posts & Telecommunications (NJUPT), Nanjing 210023, P. R. China

Experiment Section

Materials

Citric acid (99.5%) and graphite (99.95%) were purchased from Macklin. Ethylenediamine (AR) was obtained from Aladdin. Potassium hypermanganate (99.5%) was obtained from Tianjin Xintong Fine Chemical Co.. Hydrochloric acid (36%), hydrogen peroxide (30%), phosphoric acid (75%) and sulfuric acid (95%) were purchased from Liaoning Quanrui Reagent Co..

Preparation of CC and GCC

The commercial cotton fabric was washed to get rid of surface pollutants using distilled water and ethanol, and then it was dried at 60 °C. Then, cotton fabric was heated for 3 h at 700 °C in a nitrogen environment to produce CC. For the GCC, graphene oxide (GO) was prepared as previously reported at first. Classic, 2 g of graphite was slowly added into 27 mL of phosphoric acid, and then 240 mL of sulfuric acid was slowly added under mechanical mixing conditions. After that, 12 g of potassium hypermanganate was slowly put into the mixing solution. After reaching 50 °C, the mixture was stirred constantly for 12 h. After cooling to room temperature, 270 mL DI water with 10 mL hydrogen peroxide mixed solution was frozen into ice, and then the above solution was poured into ice. After that, the solution was washed with a mixture of water and hydrochloric acid, the product was separated using centrifugation, and then washed with DI water until the pH value becomes neutral. The resulting product was freeze-dried to obtain GO. After vigorous stirring and ultrasonicating, GO was disseminated in deionized water to produce the GO solution (2 mg mL^{-1}). The obtained cotton cloth (25 × 25 cm^2) was wetted by ethanol, then sprayed 60 mL GO solution evenly on the cloth with a spray bottle. Finally, it was dried for 12 h at 60 °C. Meanwhile, the color of cotton cloth changed from white to gray. For the purpose of the GCC, the cloths were heated for 3 h at 700 °C in a nitrogen environment. (i.e., 700-GCC). For 500-GCC and 900-GCC, the annealing temperatures were changed to 500 °C and 900 °C, respectively.

Preparation of CPDs-GCC

CPDs was prepared as previously reported. 6.3 g citric acid was dissolved in 60 mL DI water, stirred to dissolve and 2 mL ethylenediamine was added. After thoroughly stirring, the solution was transferred into a polytetrafluoroethylene reactor at 200 °C for 5 h. The resulting solution was freeze-dried to obtain CPDs. The above mentioned GCC was cut into rectangles of approximately 3 × 1.5 cm^2 and then immersed in 10 mL CPDs aqueous solution with a concentration of 4 mg mL^{-1}, 7 mg mL^{-1} and 10 mg mL^{-1}, respectively, and then heated for 24 h at 80 °C. At last, the cloth was taken out and dried at 60 °C overnight for further use. During this process, the CPDs nanoparticle were deposited onto GCC (denoted as CPDs-GCC). For 40 mg CPDs-GCC and 100 mg CPDs-GCC, the concentration of CPDs aqueous solutions was changed to 4 mg mL^{-1} and 10 mg mL^{-1}, respectively.

The Assembly of Full Cell

$LiFePO_4$ was used as the cathode and CPDs-GCC was used as the anode to produce the complete cells. $LiFePO_4$ electrode contained 70 wt% of $LiFePO_4$ powder, 20 wt% of acetylene black, and 10 wt% of polyvinylidene fluoride (PVDF). The cathode contained 2 mg cm^{-2} of active material. Before assembly, 8 mAh cm^{-2} of Li was predeposited on CC, GCC and CPDs-GCC, respectively. A charge/discharge test was performed at 0.2 A g^{-1}.

Electrochemical Measurements

The 2032-type coin cells were manufactured in this study utilizing a Li foil counter/reference electrode, the CC, GCC, or CPDs-GCC with a diameter of 12 mm as the working electrode. Cells were assembled in an Ar-filled glove box with water and oxygen values less than 0.01 ppm. Each coin cell used 100 μL of the electrolyte (LS-002), which was purchased from DoDoChem. The batteries was tested on LAND testing system and NEWARE testing system.

Material Characterizations

Transmission Electron Microscope (TEM) (JEM-2010F) was used to examine the shape and structure of the produced CPDs and CPDs-GCC. Using Mg Kα Excitation (1253.6 EV), the VG ESCALAB MKII spectrometer was utilized to examine X-ray Photoelectron Spectroscopy (XPS) data. Using in situ optical microscopy, the formation of lithium dendrites was monitored in real time. Using a Scanning Electron Microscope (SEM) (XL 30, ESEM-FEG, FEI Company), the morphology of the lithium coating on the surface of a lithium metal anode and anode material was described. Fourier transform infrared spectroscopy was employed to ensure the functional group on the surface of CPDs. Confocal laser scanning microscopy was used to characterize the fluorescence signal of CPDs-GCC. Electrochemical workstation (CHI660, Shanghai Chenhua Instrument Co.) was employed to test electrochemical impedance spectroscopy (EIS), i-t test and chronoamperometry test. The structures of CPDs and CPDs-GCC were characterized by using an Raman spectrum.

Theoretical calculation

All calculations were performed using the Vienna Ab Initio Simulation Package (VASP), based on density functional theory (DFT). Core-valence interactions were described using the Projector Augmented Wave (PAW) method, and the local density was approximated with the Generalized Gradient Approximation (GGA) based on the PBE exchange-correlation functional. The Brillouin zone was sampled using the Monkhorst-Pack method. A plane-wave cutoff energy (ENCUT) of 400 eV was used, with K points optimized for convergence, ranging from $1\times1\times1$ to $3\times3\times1$. Convergence criteria for electron and ion relaxation were set to 1.0×10^{-4} eV and 1.0×10^{-3} eV, respectively, while the force convergence criterion was 0.02 eV/Å.

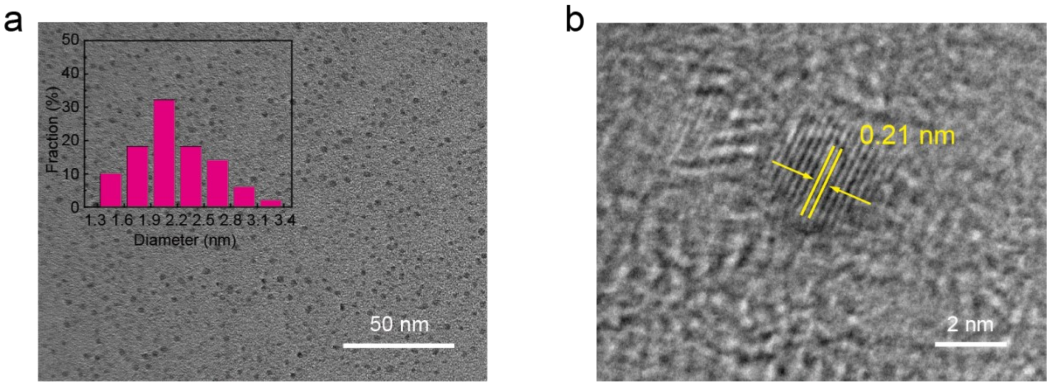

Figure S1 (a) TEM image and (b) HRTEM image of CPDs.

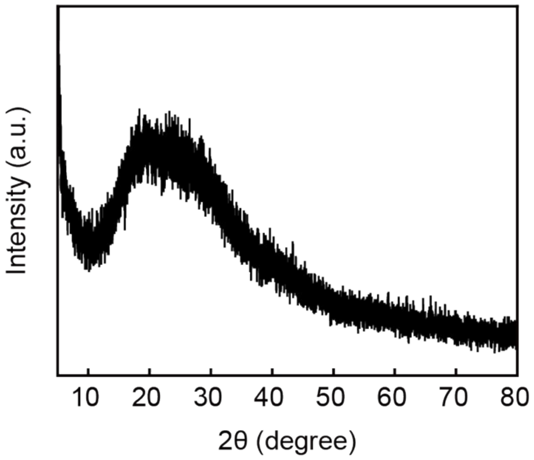

Figure S2 XRD of CPDs.

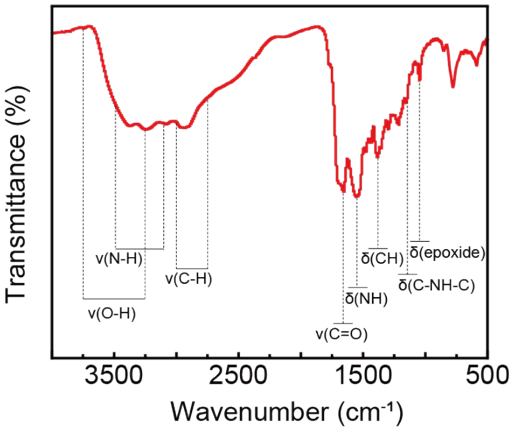

Figure S3 FT-IR spectra of CPDs.

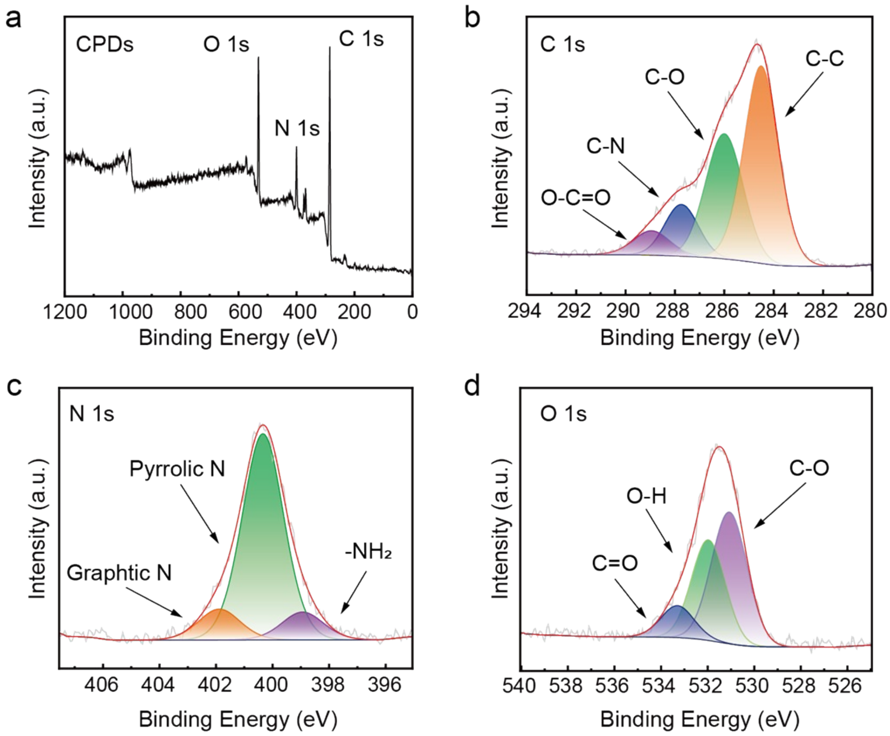

Figure S4 (a) XPS spectra of CPDs. High-resolution XPS spectra of (b) C 1s, (c) N 1s and (d) O 1s of CPDs.

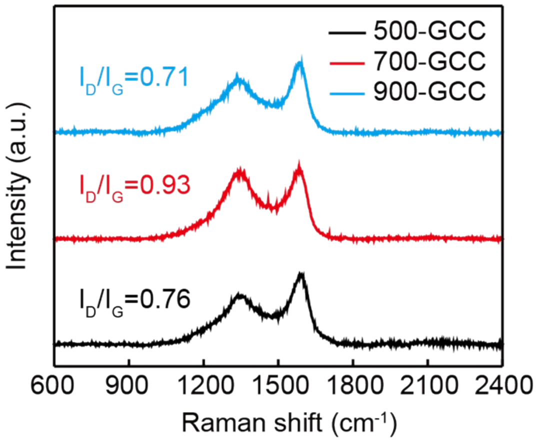

Figure S5 Raman shift of 500-GCC, 700-GCC and 900-GCC.

The impact of various annealing temperatures on GCC was examined. By annealing GO-CC for 3 h under nitrogen at 500°C, 700°C, and 900°C, 500-GCC, 700-GCC and 900-GCC were obtained. Raman spectrum shows that the ratio of I_D/I_G is 0.71, 0.93 and 0.16 for 500-GCC, 700-GCC and 900-GCC, respectively. The large value indicates the presence of more electrochemically active sites. As a result, employing 700-GCC as a substrate for the production of CPDs-GCC is advantageous for improving electrochemical performance.

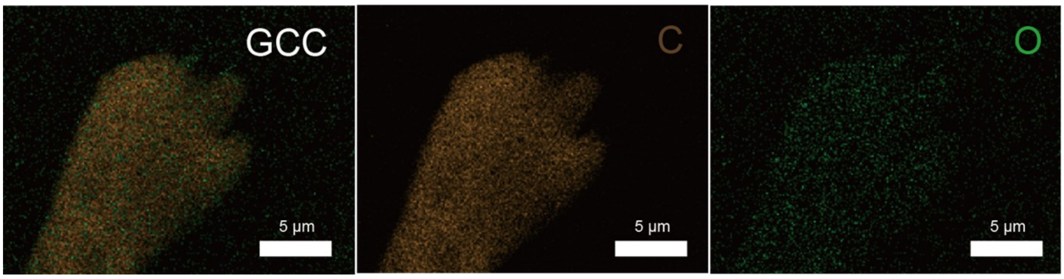

Figure S6 SEM elemental mapping images of GCC.

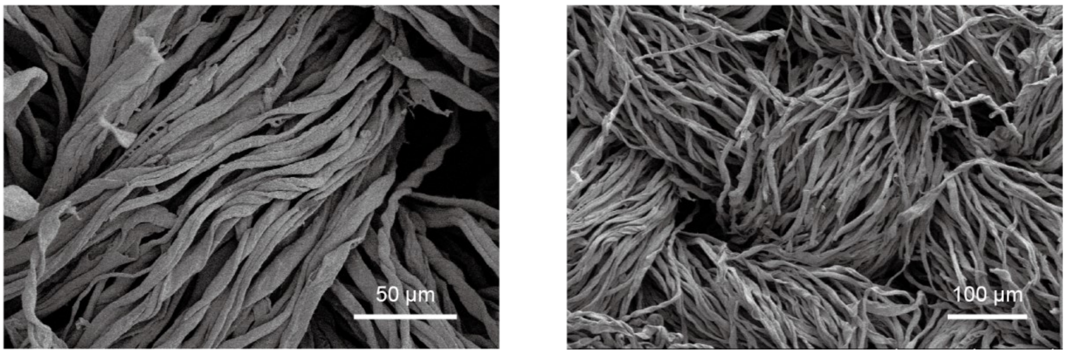

Figure S7 SEM images of CC.

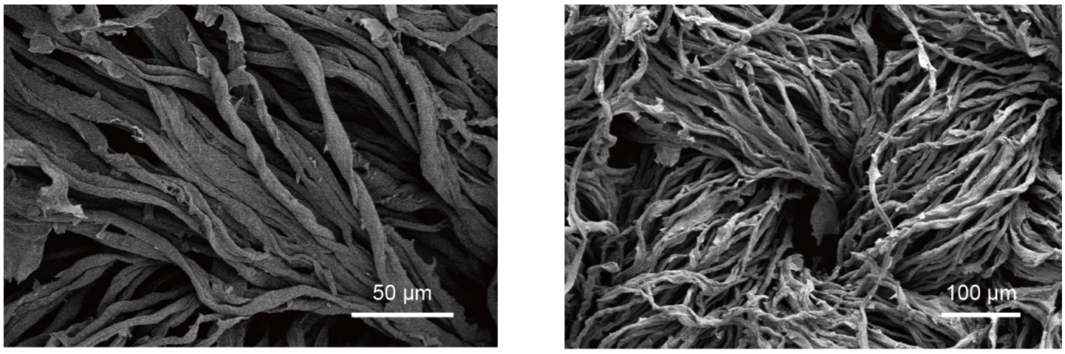

Figure S8 SEM images of GCC.

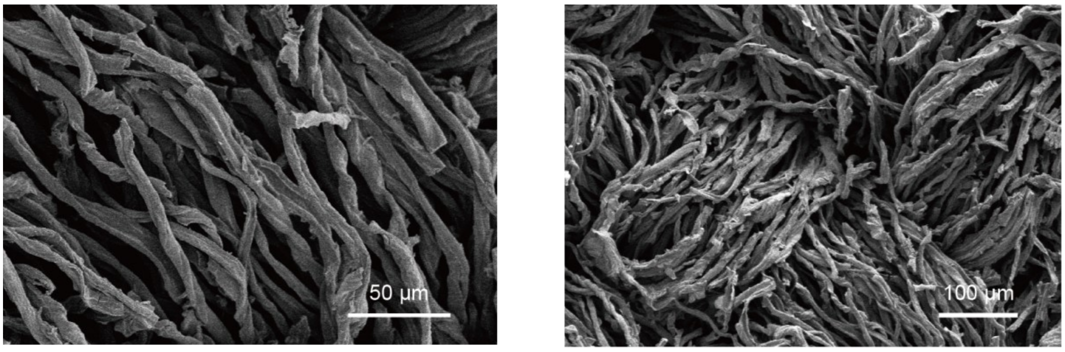

Figure S9 SEM images of CPDs-GCC.

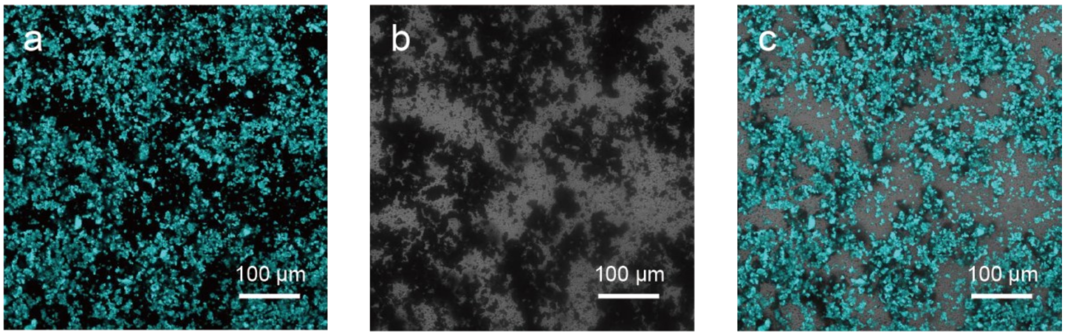

Figure S10 CLSM images of CPDs, respectively, in bright field (a), dark field (b) and compound field (c).

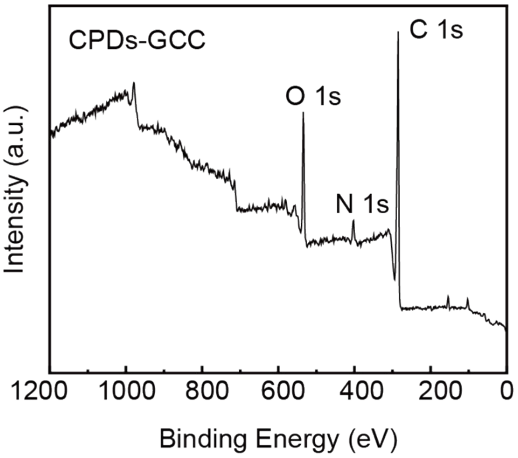

Figure S11 XPS spectra of CPDs-GCC.

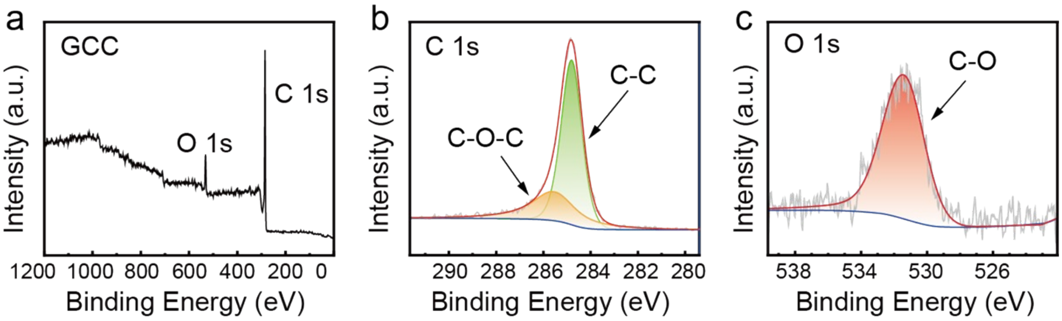

Figure S12 (a) XPS spectra of GCC. High-resolution XPS spectra of (b) C 1s and (c) O 1s of GCC.

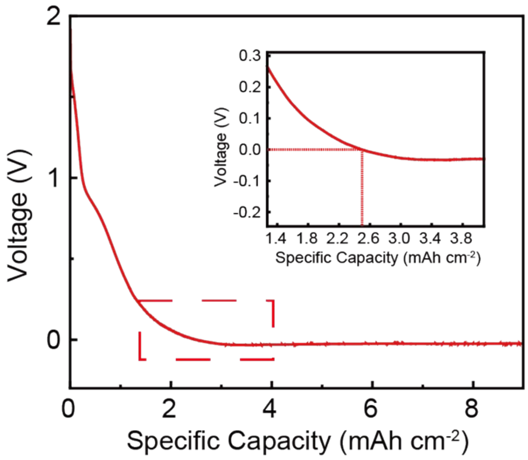

Figure S13 Li plating profile.

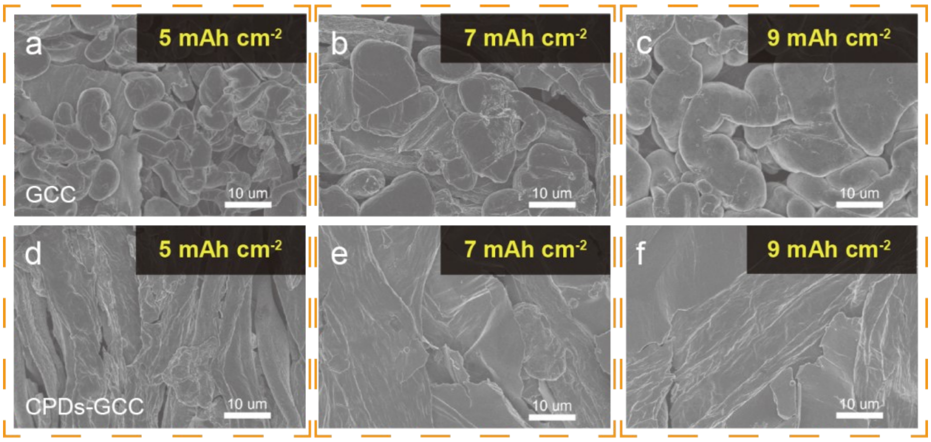

Figure S14 SEM images of GCC with Li plating to (a) 5 mAh cm^{-2} and (b) 7 mAh cm^{-2} and (c) 9 mAh cm^{-2}. SEM images of CPDs-GCC with Li plating to (d) 5 mAh cm^{-2} and (e) 7 mAh cm^{-2} and (f) 9 mAh cm^{-2}.

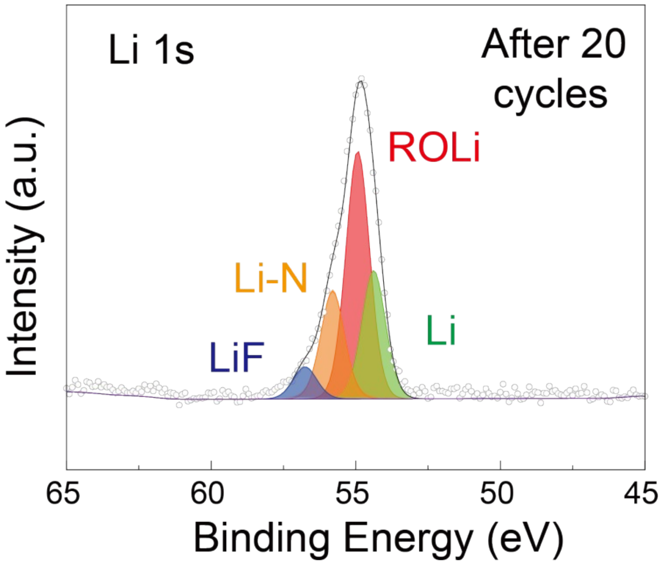

Figure S15 XPS spectrum of Li 1s for CPDs-GCC anode after 20 cycles.

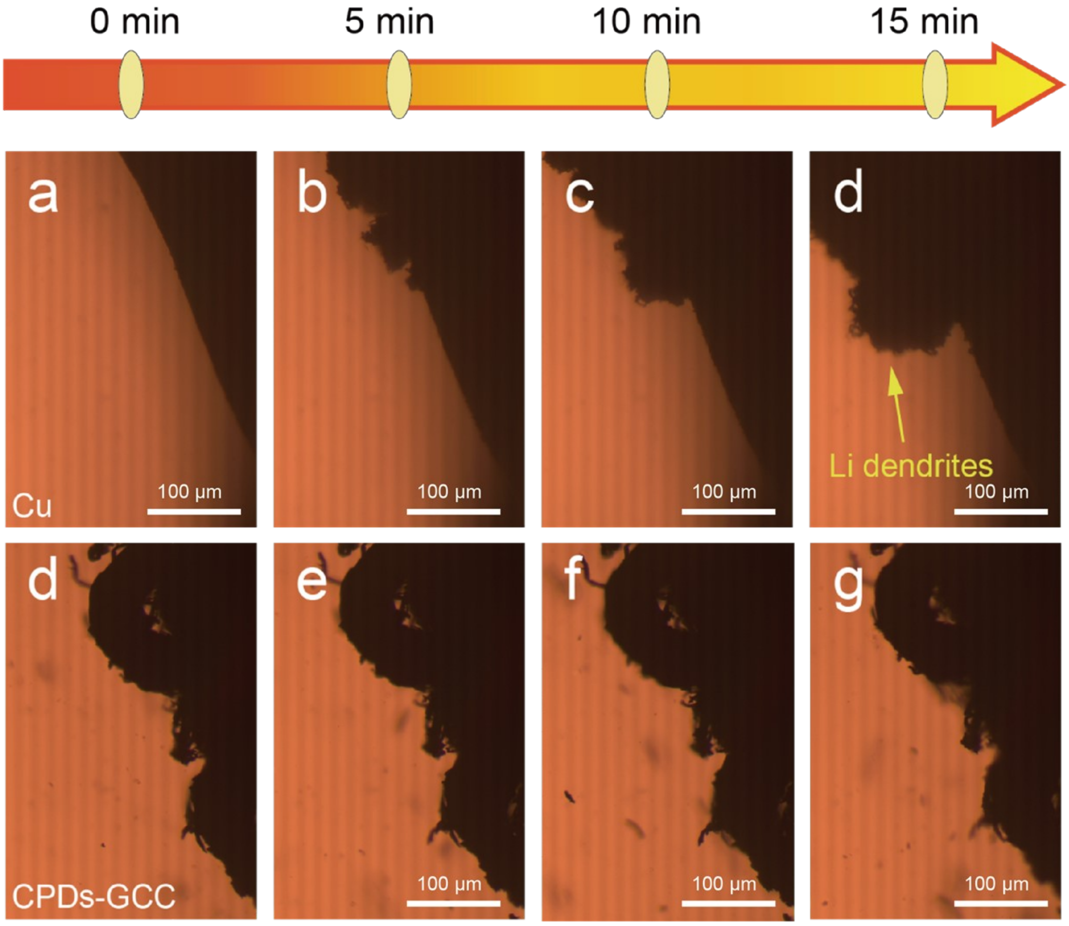

Figure S16 In-situ optical microscope image of Cu anode (a-d) and CPDs-GCC (e-h).

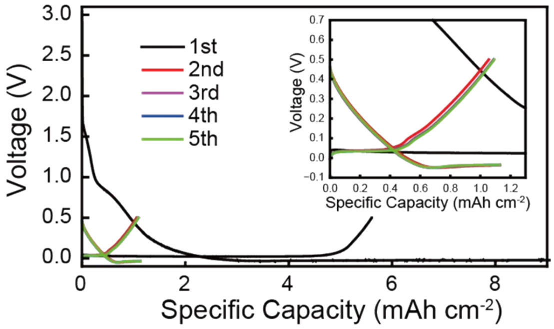

Figure S17 The charge-discharge curves for the first five cycles of CPDs-GCC at 2 mA cm^{-2} with areal capacity of 1 mAh cm^{-2}.

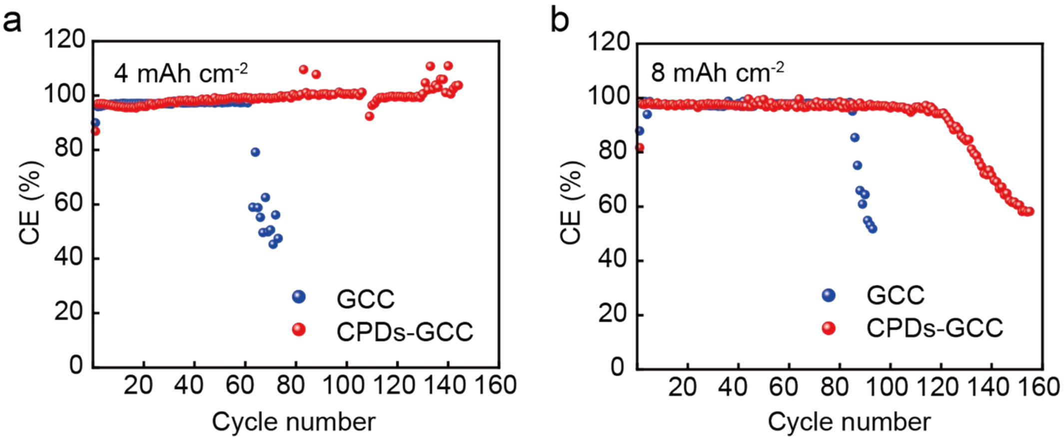

Figure S18 CE test of GCC and CPDs-GCC at areal capacity of 4 mAh cm^{-2} and 8 mAh cm^{-2} with current densities of 2 mA cm^{-2}, respectively.

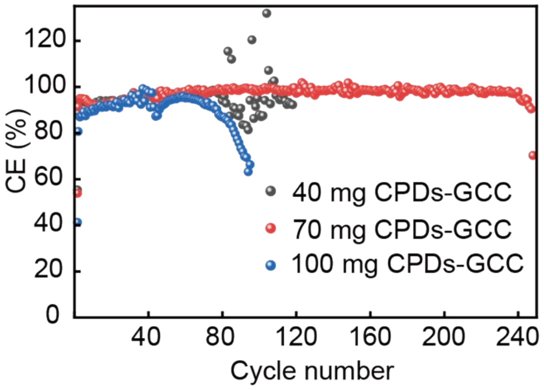

Figure S19 CE test of 40mg CPDs-GCC, 70mg CPDs-GCC 100mg CPDs-GCC at current densities of 2 mA cm^{-2} with areal capacity of 1 mAh cm^{-2}.

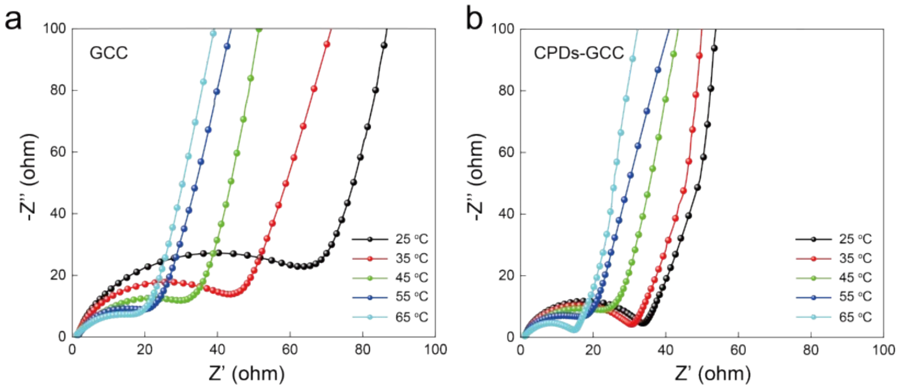

Figure S20 EIS tested at different temperatures for (a)GCC and (b) CPDs-GCC.

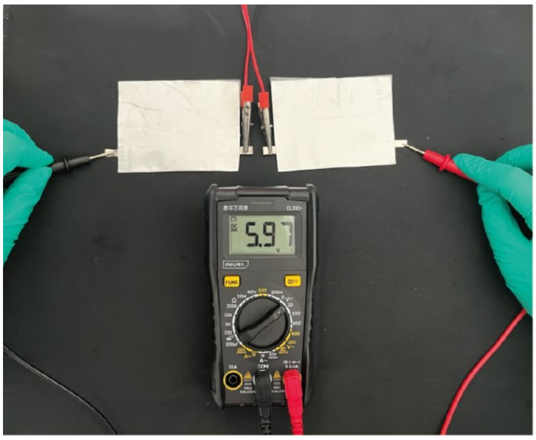

Figure S21 Voltage of two FPC series connections.

Table S1 The content of element C, O and N of CPDs.

Peak	Bending Energy (eV)	Content (%)
C 1s	284.8	71.04
N 1s	400.43	16.83
O 1s	531.66	12.13

Table S2 The content of element C, O of GCC.

Peak	Bending Energy (eV)	Content (%)
C 1s	284.8	91.06
O 1s	531.42	8.93

Table S3 The content of element C, N and O of CPDs-GCC.

Peak	Bending Energy (eV)	Content (%)
C 1s	284.8	60.73
N 1s	402.3	6.87
O 1s	533.49	32.4

Table S4 The comparison in cycling performance in this work with reported 3D structure Li metal electrodes.

Materials	Current density (mA cm^{-2})	Overpotential (mV)	Cycle time (h)	Full cell current density (A g^{-1})	Full cell cycle number	Capacity remain (%)	Ref.
CPDs-GCC	**2**	**~2**	**4800**	**0.2**	**3000**	**95**	**This work**
Li/LiZn@Cu	0.5	~9	1200	0.034	230	98	1
INf@Li	5	~82	3190	0.17	600	99	2
LMZG	1	~3	2200	0.34	400	99.79	3
VANC	1	~20	450	0.85	150	93.6	4
Li/DG-CCZ	1	~25	1000	0.17	280	91.21	5
PCHP@Li	1	~26	1000	2.26	300	84	6
OPAN/CNF	1	~18	1300	0.16	500	90.3	7
CN-NK@PP	10	~390	240	1.02	105	98.7	8
Li@GA9.25	1	~10	450	1.7	255	80	9
PP-CuPPc-S@CF	1	~44	1000	1.72	1000	81.5	10

References

1. J. Cao, Y. Shi, A. Gao, G. Du, M. Dilxat, Y. Zhang, M. Cai, G. Qian, X. Lu, F. Xie, Y. Sun and X. Lu, *Nat. Commun.*, 2024, **15**, 1354.
2. S. Xia, Z. Jiang, X. Zhao, J. A. Yuwono, X. Zhang, X. Zhang, G. Yang, J. Yang, Y. Jiang, J. Mao, K. Davey, Z. Guo and S. Zheng, *Adv. Energy Mater.*, 2024, **14**, 2304407.

3. Y. Bu, S. Huang, J. Zhu, Z. Cui, M. Gao, W. Wang and R. Zou, *J. Mater. Chem. A*, 2025, **13**, 6502-6512.
4. Y. Jin, I. Lee, T. Gu, S. Jung, H. Chang, B. Kim, J. Moon and D. Whang, *Adv. Funct. Mater.*, 2024, **34**, 2310097.
5. J. Chen, G. Liu, X. Han, H. Wu, T. Hu, Y. Huang, S. Zhang, Y. Wang, Z. Shi, Y. Zhang, L. Shi, Y. Ma, H. N. Alshareef and J. Zhao, *ACS Nano*, 2024, **18**, 13662-13674.
6. K. Lee, H. Kim, K. Ryu, K. H. Kim, J. W. Jeon, M. J. Lee, S. Kim, D. Kim, D. Shin, B. G. Kim and S. W. Lee, *J. Mater. Chem. A*, 2025, **13**, 8075-8082.
7. F. Liu, P. Zuo, J. Li, P. Shi, Y. Shao, L. Chen, Y. Tan and T. Ma, *J. Energy Chem.*, 2024, **93**, 282-288.
8. M. Bae, M. Kang and Y. Piao, *Adv. Funct. Mater.*, 2025, 2421952.
9. S. Won, A. Jung, K. Y. Lim, J. Cho, J. G. Son, H.D. Lim and B. Yeom, *Small*, 2025, **21**, 2412784.
10. M. Bae, Y. Kim, Y. Kim, Y. Chang, J. Choi, S. J. Hwang, J. S. Kim, H. S. Park, J. Lee and Y. Piao, *Energy Storage Mater.*, 2025, **75**, 104058.